ELSEVIER

Synthesis and structure of a dmpe-substituted dinuclear complex bridged by a substituent-free gallium atom: Electronic effect of metal fragment on the iron–gallium bonding

Keiji Ueno [a,*], Masakazu Hirotsu [b], Naoki Hatori [a]

[a] Department of Chemistry, Faculty of Engineering, Gunma University, Kiryu 376-8515, Japan
[b] Department of Material Science, Graduate School of Science, Osaka City University, Osaka 558-8585, Japan

Abstract

A dinuclear complex bridged by a substituent-free gallium atom, $Cp^*(dmpe)Fe-Ga-Fe(CO)_4$ (**1b**: $Cp^* = \eta\text{-}C_5Me_5$, dmpe = $Me_2PCH_2CH_2PMe_2$), was synthesized by the reaction of $Cp^*Fe(dmpe)GaCl_2$ with $K_2[Fe(CO)_4]$. Crystal structure analysis of complex **1b** showed that the geometry around the gallium atom is essentially linear and the two Fe–Ga bonds are significantly shorter than those of usual single bonds, indicating the multiple bonding character of the Fe–Ga bonds. Comparison of the structure and IR data of **1b** and those of $Cp^*(dppe)Fe-Ga-Fe(CO)_4$ (**1a**: dppe = $Ph_2PCH_2CH_2PPh_2$) revealed that the Fe–Ga bond is sensitive to the electronic character of the metal fragment. The Fe–Ga bond is shortened upon introducing a more π-basic metal fragment.
© 2006 Elsevier B.V. All rights reserved.

Keywords: Gallium iron complex; Gallylene complex; Unsaturated bonding; π-Back donation

1. Introduction

Transition metal complexes with metal-gallium unsaturated bonding have excited much recent interest from structure/bonding viewpoints [1–6]. Isolation of the first terminal gallyleneiron complex $(OC)_4FeGaAr^*$ ($2 : Ar^* = 2, 6\text{-}(2, 4, 6\text{-}Pr^i_3C_6H_2)_2C_6H_3$) by Robinson et al. triggered the extensive debate on the bonding model for the iron–gallium bond [7]. The question is whether the GaR fragment is bound via a multiple bond to the metal (e.g. $L_nM=GaR$ or $L_nM\equiv GaR$) or via a donor–acceptor interaction (e.g. $L_nM \leftarrow GaR$) [7,8]. Theoretical study by Frenking et al. suggested that the M-ER (M = metal, E = group-13 element) bond in transition metal complexes with terminal group-13 diyl ligands is mainly ionic, but is significantly affected by the π back donation from metal to ER group [9]. Several recent experimental and theoretical studies also

support this description [10,11]. However, systematic, experimental studies to investigate the electronic effect of metal fragment on the metal-gallium unsaturated bonding have been hampered by the difficulty of synthesis of such complexes.

In our previous paper, we reported synthesis and structure of the first dinuclear complex bridged by a substituent-free gallium atom $Cp^*(dppe)Fe-Ga-Fe(CO)_4$ (**1a**: $Cp^* = \eta\text{-}C_5Me_5$, dppe = $Ph_2PCH_2CH_2PPh_2$) [12]. Complex **1a** is unique since, based on the 18-electron rule, the bonding of **1a** can be described as $Cp^*(dppe)Fe-Ga=Fe(CO)_4$, i.e., a single bond between $Cp^*(dppe)Fe$ and Ga and a double bond between Ga and $Fe(CO)_4$. On contrary to the formal bonding description, structure analysis revealed that the former is even shorter than the latter. This finding indicates that the iron–gallium bonds bear considerable multiple bond character and is significantly affected by the π-back donation from the metal fragment. This also suggests that introduction of a more π-basic metal fragment should shorten the corresponding Fe–Ga bond.

* Corresponding author. Tel./fax: +81 277 30 1260.
 E-mail address: ueno@chem.gunma-u.ac.jp (K. Ueno).

In this paper, we report synthesis of a dmpe-substituted complex $Cp^*(dmpe)Fe-Ga-Fe(CO)_4$ (**1b**: dmpe = Me_2-$PCH_2CH_2PMe_2$). Comparison of the structures of complex **1a** and **1b** clearly shows that the Fe–Ga bonding is sensitive to the electronic character of the metal fragment.

2. Results and discussion

2.1. Synthesis of [Cp*(dmpe)FeGaCl₂] (3)

The target complex $Cp^*(dmpe)Fe-Ga-Fe(CO)_4$ (**1b**) was synthesized by a salt elimination reaction between a dichlorogallyliron complex $Cp^*(dmpe)FeGaCl_2$ (**3**) and $K_2[Fe(CO)_4]$ (**4**) (vide infra). The dichlorogallyl complex **3** was prepared by photochemical substitution of carbonyl groups in $Cp^*Fe(CO)_2GaCl_2$ (**5**) by dmpe in 22% yield (Eq. (1)).


$$(1)$$
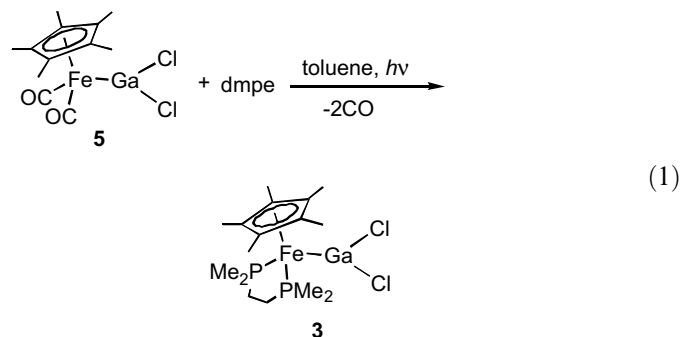
Monitoring the reaction by NMR spectroscopy demonstrated that the reaction proceeds via two intermediates. Intermediate **A** was formed when dmpe was added to a toluene-d_8 solution of **5**. ^{31}P NMR spectrum of the reaction mixture showed two signals at -26.8 and -45.2 ppm in addition to that for the free dmpe. The former is in the range of gallium-coordinated phosphines ($-20 \sim -30$ ppm) [13] whereas the later is close to that of the free dmpe. This suggests that one of the two phosphino groups in dmpe is bound to the gallium atom of gallyliron complex **5** to give complex **A** depicted in Scheme 1. When the mixture was irradiated, two new ^{31}P NMR signals appeared gradually at $+34.6$ and -41.7 ppm, which are assignable to the iron- and gallium-coordinated phosphino groups of complex **B**, respectively (Scheme 1) [13,14]. Prolonged
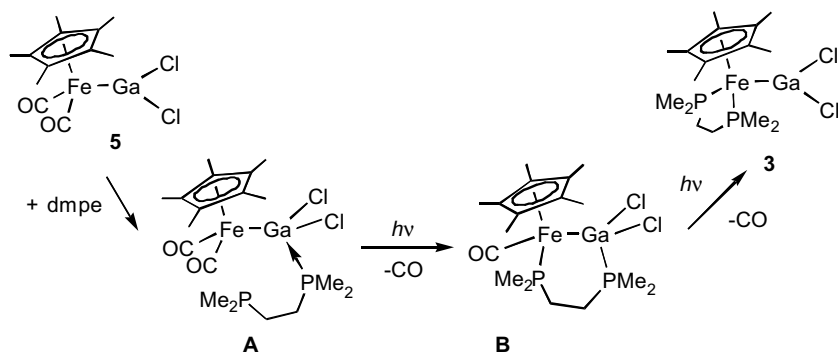
irradiation caused a decrease of the signals for the intermediates **A** and **B** and an increase of the signal at $+68.7$ ppm, which is assignable to complex **3**.

2.2. Synthesis and structure of Cp*(dmpe)Fe–Ga–Fe(CO)₄ (1b)

Reaction of the dmpe-substituted dichlorogallyliron complex $Cp^*Fe(dmpe)GaCl_2$ (**3**) with $K_2[Fe(CO)_4]$ (**4**) in THF afforded the dinuclear complex bridged by a substituent-free gallium atom, $Cp^*(dmpe)Fe-Ga-Fe(CO)_4$ (**1b**) (Eq. (2)). Complex **1b** was isolated as orange crystals in 51% yield, and fully characterized by NMR, IR spectroscopy, elemental analysis, and crystal structure analysis.

$$(2)$$
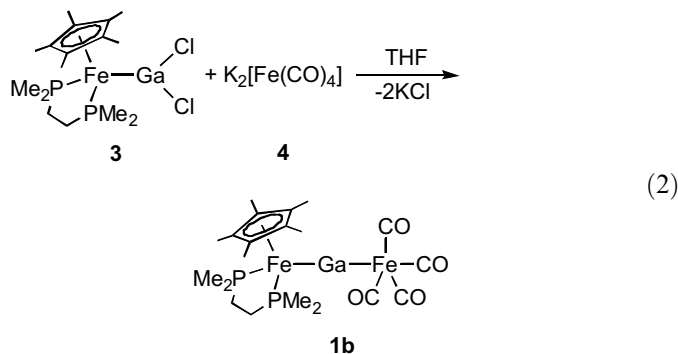
^1H NMR spectrum of complex **1b** showed Cp^* and two Me signals at 1.55, 0.66 and 1.23 ppm, respectively. Methylene proton signals of the dmpe ligand appeared at 1.45 and 1.55 ppm. The latter was overlapped with the Cp^* signal, which was confirmed by ^1H–^1H COSY NMR experiment. ^{13}C NMR spectrum of **1b** showed one CO signal, indicating fluxional behavior of four carbonyl groups in the complex.

X-ray crystal structure analysis revealed that the structure of **1b** (Fig. 1, Table 1) is similar to that of $Cp^*(dppe)Fe-Ga-Fe(CO)_4$ (**1a**) [12]. The geometry around the gallium atom is essentially linear (178.01(4)°), indicating sp-hybridization of the gallium atom. The Fe–Ga bonds (Fe(1)–Ga 2.3205(5) and Fe(2)–Ga 2.2409(5) Å) are markedly shorter than those of usual Fe–Ga single bonds (2.36–2.46 Å) [2] and comparable to those of terminal gallyleneiron complex **2** (2.2248(7) Å) [7] and a cationic
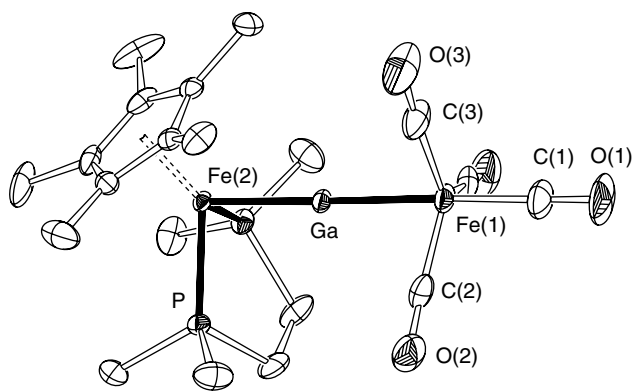

Scheme 1.

Fig. 1. ORTEP drawing of **1b** (thermal ellipsoids at the 50% probability level). Hydrogen atoms are omitted for clarity.

diiron complex bridged by a gallium atom [{Cp*Fe(CO)$_2$}$_2$(μ-Ga)]$^+$ (2.272(1) and 2.266(1) Å) [10]. These structural features indicate that the Fe–Ga bonds in **1b** bear multiple bond character.

2.3. Fe–Ga bonding in Cp*(L)Fe–Ga–Fe(CO)$_4$ (L = dppe (**1a**), dmpe (**1b**))

Table 2 summarizes the Fe–Ga bond lengths and carbonyl-stretching frequencies (vCO) of complex **1a** [12] and **1b**. Based on the 18-electron rule, bonding of **1** can be depicted as **A** in Scheme 2. However, the Cp*(L)Fe–

Table 1
Bond lengths (Å) and angles (°) for **1b**

Fe(1)–Ga	2.3205(5)	Fe(2)–Ga	2.2409(5)
P–Fe(2)	2.1678(6)	C(1)–Fe(1)	1.786(4)
C(2)–Fe(1)	1.780(4)	C(3)–Fe(1)	1.774(3)
C(1)–O(1)	1.153(5)	C(2)–O(2)	1.152(6)
C(3)–O(3)	1.158(4)		
Fe(2)–Ga–Fe(1)	178.63(2)	P–Fe(2)–Ga	90.75(2)
C(3)–Fe(1)–C(2)	118.88(9)	C(3)–Fe(1)–C(1)	96.21(11)
C(2)–Fe(1)–C(1)	94.8(2)	C(3)–Fe(1)–Ga	82.65(8)
C(2)–Fe(1)–Ga	87.50(13)	C(1)–Fe(1)–Ga	177.70(15)
P#1–Fe(2)–P	83.45(3)	O(1)–C(1)–Fe(1)	179.2(5)
O(2)–C(2)–Fe(1)	176.8(4)	O(3)–C(3)–Fe(1)	177.6(2)

Symmetry transformations used to generate equivalent atoms: #1 x, $-y + 1/2$, z.

Table 2
Comparison of Fe–Ga bond lengths and vCO frequencies of Cp*(L)Fe–Ga-Fe(CO)$_4$ (L = dppe (**1a**), dmpe (**1b**))

	Cp*(dppe) Fe–Ga-Fe(CO)$_4$ (**1a**)	Cp*(dmpe) Fe–Ga-Fe(CO)$_4$ (**1b**)
Bond lengths		
Cp*(L)Fe–Ga/Å	2.2479(10)	2.2409(5)
(CO)$_4$Fe–Ga/Å	2.2931(10)	2.3205(5)
vCO frequencies		
v/cm^{-1}	1998	1991
	1923	1917
	1890	1882
	1878	1869

Ga bond is shorter than the usual single bond. The Cp*(L)Fe–Ga bond in **1** is even shorter than the formal double bond of (OC)$_4$Fe–Ga. The remarkable shortening of the Cp*(L)Fe–Ga bond is attributable to the contribution of stronger π-back donation from the electron-rich Cp*(L)Fe fragment in comparison to that from the Fe(CO)$_4$ fragment. This bonding scheme suggests that the Fe–Ga bond lengths should be sensitive to the π-basicity of the metal fragments in the molecule. Indeed, replacing the dppe ligand of **1a** with a more electron-donating dmpe ligand in **1b** caused contraction of the Cp*(L)Fe–Ga bond (Table 2). The strong back-donation from Cp*(dmpe)Fe to Ga suppresses that from Fe(CO)$_4$, which results in the elongation of the (OC)$_4$Fe–Ga bond in **1b** compared to that of **1a**. The red shift of vCO bands of **1b** compared to those of **1a** is consistent with this interpretation. This result clearly shows that the metal-gallium bonding is significantly affected by the π-back bonding from metal to unsaturated gallium atom and, thus, contribution of a canonical form **B** is dominant for complex **1** (Scheme 2).

3. Experimental

3.1. General procedures

All manipulations were performed using either standard Schlenk tube techniques under nitrogen, vacuum line techniques, or a dry box under nitrogen. K$_2$[Fe(CO)$_4$] (**4**) [15] and Cp*Fe(CO)$_2$GaCl$_2$ (**5**) [16] were prepared by the literature methods. Toluene and THF were dried by refluxing over sodium benzophenone ketyl followed by distillation under a nitrogen atmosphere. NMR spectra were recorded on a JEOL JNM-AL300 Fourier transform spectrometer at room temperature. IR spectra were obtained on a JASCO FT/IR-600 Plus spectrometer at room temperature. Photolysis was carried out by using an Ushio UV-452 450W medium pressure Hg lamp and a Pyrex reaction vessel.

3.2. Cp*Fe(dmpe)GaCl$_2$ (**3**)

A toluene solution (15 mL) of Cp*Fe(CO)$_2$GaCl$_2$ (**5**) (0.10 g, 0.28 mmol) and dmpe (0.041 g, 0.28 mmol) placed in a Pyrex sample tube with a Teflon vacuum valve was irradiated with a 450 W medium pressure Hg lamp at 4 °C. The reaction mixture was periodically degassed by conventional freeze–pump–thaw cycles on a vacuum line. After 1.5 h, the reaction mixture was concentrated to ca. 5 mL and cooled to −30 °C to give orange crystals of Cp*Fe(dmpe)GaCl$_2$ (**3**). Yield: 0.030 g (0.062 mmol, 22%). ^{1}H NMR (300 MHz, C$_6$D$_6$) δ/ppm 1.58 (s, 15H, Cp*), 1.58 (br, 2H, CH$_2$), 1.50 (m, 6H, Me), 1.08 (m, 2H, CH$_2$), 0.72 (m, 6H, Me). ^{13}C NMR (75.5 MHz, C$_6$D$_6$) δ/ppm 85.1 (s, C_5Me$_5$), 32.2 (dd, $^1J_{PC}$ = 21 Hz, $^2J_{PC}$ = 21 Hz, PCH$_2$), 22.2 (dd, $^1J_{PC}$ = 18 Hz, $^4J_{PC}$ = 15 Hz, PMe), 20.7 (dd, $^1J_{PC}$ = 8 Hz, $^4J_{PC}$ = 6 Hz, PMe), 11.8 (s, C$_5$Me$_5$). ^{31}P NMR (121.5 MHz, C$_6$D$_6$) δ / ppm 69.0 (dmpe). Anal. Calc.
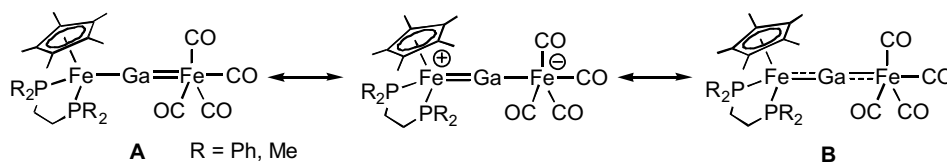
Scheme 2.

for $C_{16}H_{31}FeGaCl_2P_2$; C: 39.88, H: 6.49%. Found; C: 40.10, H: 6.32%.

3.3. $Cp^*(dmpe)Fe$–Ga–$Fe(CO)_4$ (1b)

A suspension of $K_2[Fe(CO)_4]$ (4) (0.036 g, 0.15 mmol) in THF (5 mL) was added slowly to $Cp^*Fe(dmpe)GaCl_2$ (3) (0.065 g, 0.13 mmol) in THF (5 mL) at room temperature with vigorous stirring. The solution was stirred for 1 h and then filtered through a glass filter. The filtrate was concentrated to ca. 2 mL and cooled to −30 °C to give orange precipitates. Recrystallization of the precipitates using a small amount of toluene gave orange crystals of $Cp^*(dmpe)Fe$–Ga–$Fe(CO)_4$ (1). Yield: 0.040 g (0.069 mmol, 51%). ^{1}H NMR (300 MHz, C_6D_6) δ/ppm 1.55 (s, 15H, Cp*), 1.55 (br, 2H, CH_2), 1.41 (m, 6H, Me), 1.23 (m, 2H, CH_2), 0.66 (m, 6H, Me). ^{13}C NMR (75.5 MHz, C_6D_6) δ/ppm 218.9 (s, CO), 85.7 (s, C_5Me_5), 32.7 (dd, $^1J_{PC} = 23$ Hz, $^2J_{PC} = 23$ Hz, PCH_2), 24.5 (dd, $^1J_{PC} = 15$ Hz, $^4J_{PC} = 15$ Hz, PMe), 20.2 (dd, $^1J_{PC} = 8$ Hz, $^4J_{PC} = 8$ Hz, PMe), 11.3 (s, C_5Me_5). ^{31}P NMR (121.5 MHz, C_6D_6) δ / ppm 65.8 (dmpe). IR (KBr) v/cm^{-1} 1991, 1917, 1882, 1869 (vCO). Anal. Calc. for $C_{20}H_{31}Fe_2GaO_4P_2$; C: 41.50, H: 5.40%. Found; C: 41.26, H: 5.37%.

3.4. X-ray crystal structure determination of $Cp^*(dmpe)Fe$–Ga–$Fe(CO)_4$ (1b)

A single crystal suitable for X-ray crystal structure determination was mounted on a glass fiber. The intensity data were collected on a RIGAKU RAXIS-IV Imaging Plate diffractometer with graphite monochromated Mo Kα radiation at 133 K. Crystallographic data are listed in Table 3. The structure was solved by direct and Fourier transform methods using SHELX-97 [17]. All non-hydrogen atoms were refined by full-matrix least-squares techniques with anisotropic displacement parameters based on F^2 with all reflections. All hydrogen atoms were placed at their geometrically calculated positions and refined riding on the corresponding carbon atoms with isotropic thermal parameters. The final residue R_1 and the weighted wR_2 were 0.0593 and 0.1461, respectively.

Acknowledgements

Appendix A. Supplementary data

CCDC 299567 contains the supplementary crystallographic data for this paper. These data can be obtained free of charge from The Cambridge Crystallographic Data Centre via www.ccdc.cam.ac.uk/data_request/cif. Supplementary data associated with this article can be found, in the online version, at doi:10.1016/j.jorganchem.2006.08.052.

Table 3
Crystal data and structure refinement for complex **1b**

Complex	**1b**
Empirical formula	$C_{20}H_{31}Fe_2GaO_4P_2$
Formula weight	578.81
Temperature (K)	133(2)
Wavelength (Å)	0.71073
Crystal system	Orthorhombic
Space group	*Pnma*
Unit cell dimensions	
a (Å)	16.5848(11)
b (Å)	13.3328(9)
c (Å)	11.1504(9)
Volume (Å^3)	2465.6(3)
Z	4
D_{calc} (Mg/m^3)	1.559
Absorption coefficient	2.398 mm^{-1}
$F(000)$	1184
Crystal size (mm^3)	$0.35 \times 0.25 \times 0.22$
θ Range for data collection (°)	2.20–32.28
Index ranges	$-24 \leqslant h \leqslant 19$, $-18 \leqslant k \leqslant 18$, $-15 \leqslant l \leqslant 11$
Reflections collected	10713
Independent reflections [R_{int}]	3872 [0.0252]
Absorption correction	Semi-empirical from equivalents
Maximum and minimum transmission	1.0000 and 0.5655
Refinement method	Full-matrix least-squares on F^2
Data/restraints/parameters	3872/0/146
Goodness-of-fit on F^2	1.070
Final R indices [$I > 2\sigma(I)$]	$R_1 = 0.0593$, $wR_2 = 0.1461$
R indices (all data)	$R_1 = 0.0599$, $wR_2 = 0.1469$
Largest difference in peak and hole (e Å^{-3})	0.679 and −2.106

References

[1] (a) H. Braunschweig, Angew. Chem., Int. Ed. Engl. 37 (1998) 1882;
    (b) H. Braunschweig, J. Colling, Eur. J. Inorg. Chem. (2003) 383;
    (c) H. Braunschweig, M. Colling, Coord. Chem. Rev. 223 (2001) 1.
[2] R.A. Fischer, J. Weiss, Angew. Chem., Int. Ed. Engl. 38 (1999) 2830.

[3] G. Linti, H. Schnockel, Coord. Chem. Rev. 206 (2000) 285.

[4] T.R. Cundari, Chem. Rev. 100 (2000) 807.

[5] J.W. Herndon, Coord. Chem. Rev. 248 (2002) 3.

[6] W. Uhl, M. Benter, S. Melle, W. Saak, Organometallics 18 (1999) 3778.

[7] J. Su, X.-W. Li, R.C. Crittendon, C.F. Campana, G.H. Robinson, Organometallics 16 (1997) 4511.

[8] F.A. Cotton, X. Feng, Organometallics 17 (1998) 128.

[9] (a) J. Uddin, C. Boehme, G. Frenking, Organometallics 19 (2000) 571;
(b) C. Boehme, G. Frenking, Chem. Eur. J. 5 (1999) 2184;
(c) J. Uddin, G. Frenking, J. Am. Chem. Soc. 123 (2001) 1683.

[10] (a) N.R. Bunn, S. Aldridge, D.L. Coombs, A. Rossin, D.J. Willock, C. Jones, L. Ooi, Chem. Commun. (2004) 1732;
(b) N.R. Bunn, S. Aldridge, D.L. Kays, N.D. Coombs, A. Rossin, D.J. Willock, J.K. Day, C. Jones, L. Ooi, Organometallics 24 (2005) 5891;

(c) S. Aldridge, A. Rossin, D.L. Coombs, D.J. Willock, Dalton Trans. (2004) 2649.

[11] (a) X.J. Yang, Y. Wang, B. Quillian, P. Wei, Z. Chen, P.v.R. Schleyer, G.H. Robinson, Organometallics 25 (2006) 925;
(b) X.J. Yang, B. Quillian, Y. Wang, P. Wei, G.H. Robinson, Organometallis 23 (2004) 5119.

[12] K. Ueno, T. Watanabe, H. Tobita, H. Ogino, Organometallics 22 (2003) 4375.

[13] C. von Hänisch, P. Scheer, B. Rolli, Eur. J. Inorg. Chem. 12 (2002) 3268.

[14] R.A. Paciello, J.M. Manriquez, J.E. Bercaw, Organometallics 9 (1990) 260.

[15] J.A. Gladysz, W. Tam, J. Org. Chem. 43 (1978) 2279.

[16] K. Ueno, T. Watanabe, H. Ogino, Appl. Organomet. Chem. 17 (2003) 403.

[17] G.M. Sheldrick, SHELX-97, Program for Crystal Structure Determination, University of Göttingen, Göttingen, Germany, 1997.